PRAMANA — journal of physics

Vol. 84, No. 5
May 2015
pp. 671–684

Thermalization and isotropization in heavy-ion collisions

MICHAEL STRICKLAND
Physics Department, Kent State University, Kent, OH 44242, USA
E-mail: mstrick6@kent.edu

DOI: 10.1007/s12043-015-0972-1; ***e*Publication:** 1 May 2015

Abstract. Our current understanding of the processes driving the thermalization and isotropization of the quark gluon plasma (QGP) created in ultrarelativistic heavy-ion collisions (URHICs) is reviewed. Initially, the phenomenological evidence in favour of the creation of a thermal but momentum–space anisotropic QGP in URHICs is discussed. Further, the degree of isotropization using viscous (dissipative) hydrodynamics, weak-coupling approaches to QGP dynamics, and strong-coupling approaches to QGP dynamics are discussed. Finally, recent progress in the area of real-time non-Abelian gauge field simulations and non-Abelian Boltzmann–Vlasov-based hard-loop simulations are reported.

Keywords. Quark gluon plasma; thermalization; isotropization; heavy-ion collisions.

PACS Nos 11.15.Bt; 11.10.Wx; 12.38.Mh; 25.75.−q; 52.27.Ny; 52.35.−g

1. Introduction

In this brief review our current understanding of the thermalization and isotropization of the quark gluon plasma (QGP) created in relativistic heavy-ion collisions is summarized. This is still very much an active area of research and, as such, there remain many open questions; however, much has been learned, both on the theoretical and phenomenological fronts since the first $\sqrt{s_{NN}} = 200$ MeV Au–Au data were made available from Au–Au collisions at the Relativistic Heavy Ion Collider (RHIC) at Brookhaven National Laboratory over a decade ago. In the interim, the heavy-ion community has collected a tremendous amount of experimental data and our theoretical understanding, both in terms of our ability to simulate the non-Abelian dynamics of the QGP from first principles and to model the QGP based on effective models, has advanced tremendously. Additionally, with the turn-on of the Large Hadron Collider (LHC) at the European Center for Nuclear Research (CERN) in 2008, we now have access to $\sqrt{s_{NN}} = 2.76$ TeV Pb–Pb data which allows us to further push into the QGP part of the phase diagram of quantum chromodynamics (QCD). Looking to the future, the full energy Pb–Pb runs with $\sqrt{s_{NN}} = 5.5$ TeV will push us even further into the QGP phase. Despite this progress,

there remains an important open theoretical question in the field: How fast does the QGP thermalize/isotropize and what are the most important processes contributing to this?

There is some lingering confusion concerning the empirical evidence for fast thermalization and isotropization in the QGP. This confusion stems, in part, from phenomenological fits using ideal hydrodynamics which emerged shortly after the first RHIC data became available. The heavy-ion community interpreted the ability of ideal hydrodynamical models to describe the $p_{\rm T}$-dependence of the transverse elliptical flow as solid evidence that the QGP created in heavy-ion collisions became isotropic and thermal at approximately 0.5–1 fm/c after the initial nuclear impact [1–4]. Since the early days of ideal hydrodynamics there was a concerted effort to make hydrodynamical models more realistic by including the effect of shear and bulk viscosities (relaxation times). This has led to a proper formulation of relativistic viscous hydrodynamics [5–27] and, recently, anisotropic relativistic viscous hydrodynamics [28–39]. The conclusion one reaches from dissipative hydrodynamic approaches is that the QGP created in ultrarelativistic heavy-ion collisions (URHICs) has quite different longitudinal (along the beam line) and transverse pressures, particularly at times $\tau \lesssim 2$ fm/c.

In addition to the progress made in dissipative hydrodynamical modelling of the QGP, there have been significant advances in our understanding of the underlying quantum field theory processes driving the thermalization and (an-)isotropization of the QGP in the weak [40–64] and strong-coupling [65–76] limits. The picture emerging from these advances seems to fit nicely into the picture emerging from the aforementioned dissipative hydrodynamics findings, namely that the QGP as created in URHICs possesses large momentum–space anisotropies in the local rest frame, and is particularly anisotropic at early times after the initial nuclear impact. On the separate issue of thermalization, there is evidence from simulations of weak-coupling non-Abelian dynamics, that one can achieve rapid apparent longitudinal thermalization of the QGP due to the chromo-Weibel instability [61] (see also the early time spectra reported in ref. [57]). However, it is noted that classical Yang–Mills simulations find power-law scaling associated with turbulence emerging at late simulation times [57,77,78]. As the saturation scale depends on the strong-coupling constant, one cannot naively extrapolate these results to realistic values of the strong-coupling constant to make predictions for RHIC/LHC heavy-ion collisions; however, with more data on the dependence on initial conditions, this should be possible in the near future. On the strong-coupling front, practitioners are now able to use numerical GR to describe the formation of an extradimensional black hole (or more accurately an apparent horizon), which is the criterium for QGP thermalization in the AdS/CFT framework. In an expanding background corresponding to the (approximately) boost-invariant Bjorken-like expansion of the QGP, these studies find thermalization times that are less than 1 fm/c. However, the state which emerges is momentum–space anisotropic even in the infinite 't Hooft coupling limit. However, once again, for realistic applications, practitioners will need to relax the infinite strong-coupling and large $N_{\rm c}$ limits which is highly non-trivial.

Before proceeding to a more detailed discussion of the (an-)isotropization and thermalization of the QGP, it may be noted that URHICs are very much a data-driven field. Viscous (dissipative) hydrodynamical models can describe the collective (elliptic, triangular, etc.) flow of the QGP produced at RHIC and LHC, both in terms of event-averaged observables and their underlying probability distributions, with a surprising level of

accuracy. As viscous (dissipative) hydrodynamics implies the existence of momentum–space anisotropies in the QGP, one must now conclude, based on empirical evidence, that the QGP might be thermal but strongly anisotropic in momentum–space, implying that the QGP has two temperatures – a transverse one and a longitudinal one. The existence of such anisotropies must now be taken seriously if one is to treat the phenomenology of the QGP self-consistently. This means, in practice, that one has to fold into the calculation of various processes, e.g. photon production, dilepton production, heavy quarkonium suppression, jet suppression, etc. the momentum–space anisotropy of the underlying one-particle parton distribution functions. There have been some initial work along these lines [79–101] (see also [102–107] for recent progress along these lines using second-order viscous hydrodynamics), but there is still much work left to be done. In the process, one may find observables that are sensitive to the level of momentum–space anisotropy in the QGP, thereby allowing us to have independent confirmation of their existence outside the realm of viscous (dissipative) hydrodynamics.

2. Momentum–space anisotropies in the QGP

As discussed above, many disparate approaches to QGP dynamics consistently find that the QGP, as created in URHICs, possesses large local rest frame momentum–space anisotropies in the $p_{\rm T}$–$p_{\rm L}$ plane due to the initially rapid longitudinal expansion of the matter. As the first indication of this, let us consider relativistic viscous hydrodynamics for a system that is transversely homogeneous and boost invariant in the longitudinal direction, aka 0+1d dynamics. In this case, first-order Navier–Stokes (NS) viscous hydrodynamics predicts that the shear correction to the ideal pressures is diagonal with space-like components $\pi^{zz} = -4\eta/3\tau = -2\pi^{xx} = -2\pi^{yy}$, where η is the shear viscosity and τ is the proper time. In viscous hydrodynamics, the longitudinal pressure is given by $\mathcal{P}_{\rm L} = P_{\rm eq} + \pi^{zz}$ and the transverse pressure by $\mathcal{P}_{\rm T} = P_{\rm eq} + \pi^{xx}$. Assuming an ideal equation of state (EoS), the ratio of the longitudinal pressure to the transverse pressure from first-order viscous hydrodynamics can be expressed as

$$\left(\frac{\mathcal{P}_{\rm L}}{\mathcal{P}_{\rm T}}\right)_{\rm NS} = \frac{3\tau T - 16\bar{\eta}}{3\tau T + 8\bar{\eta}}\,, \tag{1}$$

where $\bar{\eta} \equiv \eta/\mathcal{S}$, with $\mathcal{S}$ being the entropy density. Assuming RHIC-like initial conditions with $T_0 = 400$ MeV at $\tau_0 = 0.5$ fm/c and taking the conjectured lower bound $\bar{\eta} = 1/4\pi$ [108], one finds $(\mathcal{P}_{\rm L}/\mathcal{P}_{\rm T})_{\rm NS} \simeq 0.5$. For LHC-like initial conditions with $T_0 = 600$ MeV at $\tau_0 = 0.25$ fm/c and once again taking $\bar{\eta} = 1/4\pi$, one finds $(\mathcal{P}_{\rm L}/\mathcal{P}_{\rm T})_{\rm NS} \simeq 0.35$. This means that even in the best case scenario of $\bar{\eta} = 1/4\pi$, viscous hydrodynamics itself predicts rather sizable momentum–space anisotropies. For larger values of $\bar{\eta}$, one obtains even larger momentum–space anisotropies. In addition, one can see from eq. (1) that, at fixed initial proper time, the level of momentum–space anisotropy increases as one lowers the temperature. This means, in practice, that as one moves away from the centre of the nuclear overlap region towards the transverse edge, the level of momentum–space anisotropy increases.

Of course, as first-order relativistic viscous hydrodynamics is acausal, the above analysis is not the full story. It does, however, provide important intuitive guidance as the causal second-order version of the theory has the first-order solution as an attractive 'fixed

point' of the dynamics. Because of this, one expects large momentum–space anisotropies to emerge within a few multiples of the shear relaxation time τ_π. In the strong-coupling limit of $\mathcal{N} = 4$ SYM one finds $\tau_\pi = (2-\log 2)/2\pi T$ [10,109] which gives $\tau_\pi \sim 0.1$ fm/c and $\tau_\pi \sim 0.07$ fm/c for the RHIC- and LHC-like initial conditions stated above [109a]. To demonstrate this quantitatively, in figure 1, the solution of the second-order Israel-Stewart 0+1d viscous hydrodynamical equations assuming an isotropic initial condition and the NS solution together is plotted [109b]. In figure 1a $4\pi\bar{\eta} = 1$ and in the figure 1b $4\pi\bar{\eta} = 3$ ($\bar{\eta} \simeq 0.24$) is assumed, with $\tau_\pi = 2(2 - \log 2)\bar{\eta}/T$ in both cases [110]. As can be seen from this figure, even if one starts with an isotropic initial condition, within a few multiples of the shear relaxation time, one approaches the NS solution, overshoots it, and then approaches it from below. The value of $\bar{\eta}$ in figure 1b is approximately the same as that extracted from recent fits to LHC collective flow data [111]. It is noted that, if one further increases $\bar{\eta}$, then one finds negative longitudinal pressures in second-order viscous hydrodynamics as well.

Based on the preceding discussion, one learns the value of $\bar{\eta}$ extracted from LHC data [111], which implies that the system may be highly momentum–space anisotropic with the momentum–space anisotropies persisting throughout the evolution of the QGP. However, before drawing conclusions based solely on the relativistic viscous hydrodynamics, we can ask the corresponding question within the context of the AdS/CFT framework. Several groups have been working on methods to address the question of early-time dynamics within the context of the AdS/CFT framework. Here the focus is on the work of two groups: Heller *et al* [70] and van der Schee *et al* [76]. Both of them simulated the dynamics of an expanding QGP using numerical general relativity (GR). In the work of Heller *et al* they simulated the early time dynamics of a 0+1d system by numerically solving the GR equations in the bulk. In the work of van der Schee *et al* [76], they performed similar numerical GR evolution but in the case of a 1+1d radially symmetric system including transverse expansion.

In figure 2a the Heller *et al* result for the pressure anisotropy expressed as $1 - 3\mathcal{P}_\mathrm{L}/\mathcal{E}$ is shown. In the paper from which this figure is adapted, the authors found that the evolution begins to be well-approximated by viscous hydrodynamics after a 'time' of

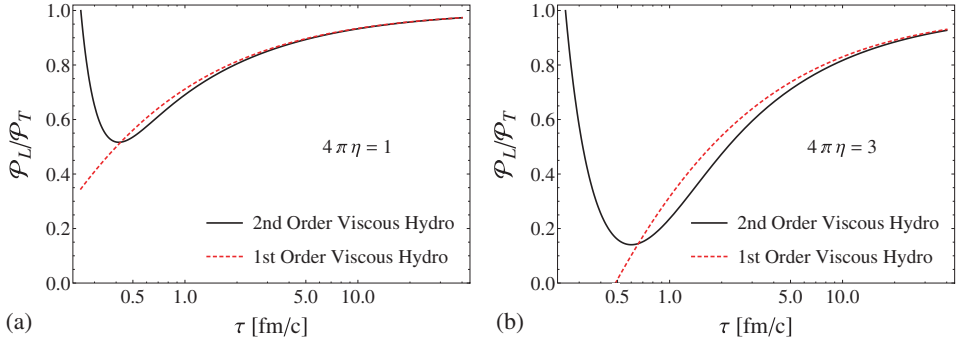

Figure 1. Pressure anisotropy as a function of proper time assuming an initially isotropic system with $T_0 = 600$ MeV at $\tau_0 = 0.25$ fm/c for $4\pi\bar{\eta} = 1$ (**a**) and 3 (**b**). Solid black line is the solution of the second-order coupled differential equations and the red dashed line is the first-order 'Navier–Stokes' solution.

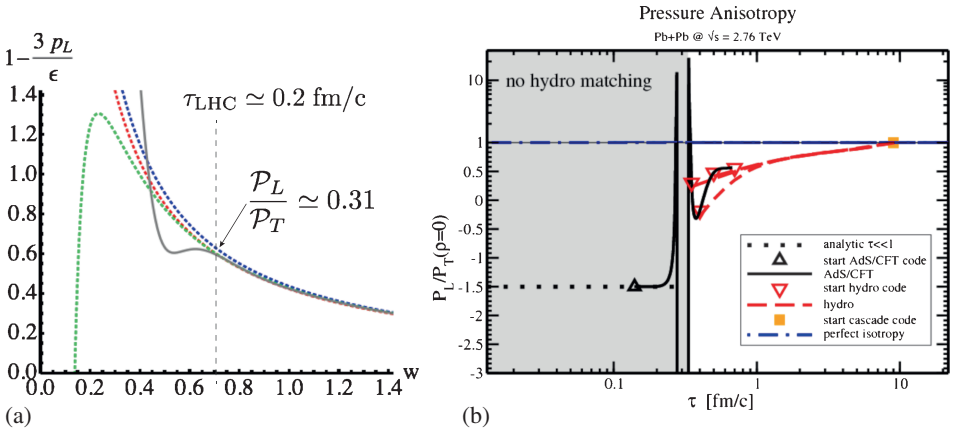

Figure 2. Pressure anisotropy as a function of proper time from two different AdS/CFT-based calculations. (**a**) Results from Heller *et al* [70] and (**b**) results from van der Schee *et al* [76] (the figure in (**a**) has been adapted to add labels).

$w = T_{\rm eff}\tau \sim 0.63$ which, upon conversion to physical units using LHC initial conditions, corresponds to $\tau \simeq 0.2$ fm/c (indicated by a vertical dashed line in the figure). The red, green, and blue dashed lines correspond to first-, second-, and third-order viscous hydrodynamics results and the grey solid line corresponds to a typical evolution within their numerical GR approach. As can be seen from this figure, the results are consistent with the estimates for the initial pressure anisotropy obtained previously. In addition, we see that the pressure anisotropy persists, decaying as an inverse power of the proper time. As the result was obtained in the context of the strong-coupling limit for which $4\pi\bar{\eta} = 1$, the pressure anisotropy obtained should be considered an upper bound. Figure 2b shows the result of van der Schee *et al*. In this figure, the shaded region on the left covers the time over which they performed a numerical GR solution which was then matched to viscous hydrodynamical evolution at the border between the grey and the white regions. As can be seen from this figure, even when including radial expansion, one obtains sizable momentum–space anisotropies which are consistent in magnitude with the 0+1d results. Once again the authors assumed $4\pi\bar{\eta} = 1$, and so the pressure anisotropy obtained should be considered an upper bound.

Having covered the degree of momentum–space anisotropy predicted by viscous hydrodynamics and the AdS/CFT approach, I would now like to briefly discuss the pressure anisotropies expected within the colour glass condensate (CGC) [112–114] framework and weakly-coupled gauge field theory in general. In the CGC framework, the fields are boost-invariant to first approximation. As a result, the leading-order prediction is that longitudinal pressure is zero [114a]. Including finite energy corrections results in a very small longitudinal pressure. Currently, it is believed that the primary driving force for restoring isotropy in the gauge field sector are plasma instabilities such as the chromo-Weibel instability [115]; however, so far practitioners have found that, even taking into account the unstable gauge field dynamics, the time-scale for isotropization of the system is very long [54,116]. The recent work of Epelbaum and Gelis [117] has included resummation of next-to-leading order (NLO) quantum loop corrections to initial CGC fluctuations, and simulations in this framework find early-time pressure anisotropies of the order of

0.01–0.5, depending on the assumed value of the strong-coupling constant $g_s = 0.1$–0.4. In the context of hard-loop simulations of chromo-Weibel instability evolution, one finds rapid thermalization of the plasma in the sense that a Boltzmann distribution of gluon modes is established within $\sim$1 fm/c (see below). However, large pressure anisotropies persist for at least 5–6 fm/c [61].

3. QGP thermalization via collective instabilities

Many processes are at play in a non-equilibrium non-Abelian plasma. These include elastic scattering, inelastic scattering, and collective instabilities. In the seminal paper of Baier, Mueller, Schiff, and Son (BMSS) [118], the first two of these were included in a self-consistent calculation of the thermalization and isotropization time of the QGP, with the authors of this paper finding that $\tau_{\rm therm} \sim \alpha_s^{-13/5} Q_s^{-1}$, where the constant of proportionality was argued to be approximately 1 [118]. Plugging in values of Q_s appropriate for RHIC and LHC energies, 1.4 GeV and 2 GeV, respectively, and boldly extrapolating to $\alpha_s = 0.3$, one finds $\tau_{\rm therm} \sim 3.2$ fm/c and 2.3 fm/c at RHIC and LHC energies, respectively. Firstly, we note that according to BMSS, this is the time-scale for full isotropization and thermalization of the plasma and so should be taken as an upper limit for the thermalization time because isotropization is much harder (if not impossible) to achieve. That being said, as mentioned above, this estimate does not include the effect of plasma instabilities and it is natural to ask how do instabilities affect the thermalization and isotropization of the QGP.

Before proceeding, let me note that in the context of heavy-ion collisions the central question which has to be addressed is that of the impact of longitudinal dynamics on the QGP. In fact, in the seminal paper of Krasnitz, Nara, and Venugopalan [119] the authors demonstrated that, within the CGC framework, there is transverse isotropization of gauge fields at times of the order of Q_s^{-1} (few fractions of a fm/c). They showed that, in the forward light cone, the Coulomb gauge-fixed spectrum of the transverse degrees of freedom was described very well by a Bose–Einstein distribution at low momenta and a logarithm-corrected power-law at high momenta. This finding implies that the soft modes are transversally isotropic and thermal at very early times due to strong gauge field self-interactions. For this reason, the key questions in URHIC thermalization concern the 'longitudinal' thermalization and, more generally, isotropization of a QGP which is (at least approximately) boost-invariant and expanding anisotropically.

The plasma instability which plays the most important role in the isotropization and thermalization of the QGP is the so-called chromo-Weibel instability [119a]. In the asymptotically weak-coupling limit, this instability is present whenever the QGP possesses a certain degree of momentum–space anisotropy. For a given momentum–space anisotropy, measured by an anisotropy parameter $\xi = \frac{1}{2}\langle p_T^2\rangle/\langle p_L^2\rangle - 1$, one finds that a band of soft modes with $k \lesssim gT_\perp$, where $T_\perp$ is the transverse temperature of the system, is initially unstable to filamentation-induced exponential growth of transverse chromomagnetic and chromoelectric fields (primary unstable modes). Due to non-Abelian interactions, these primary unstable modes rapidly generate longitudinal chromomagnetic and chromoelectric fields which grow at twice the rate as the initially-induced transverse fields [45,48,51,121,122]. The growth rate of these unstable modes

is parametrically $\Gamma_{\text{instability}} \sim gT_\perp$. Comparing this to other rates, namely the rate for elastic scattering $\Gamma_{\text{elastic}} \sim g^4 T_\perp$ and the rate for inelastic scattering and colour rotation $\Gamma_{\text{inelastic,colour}} \sim g^2 T_\perp$, we immediately see that the rate for unstable mode growth exceeds all other relevant processes in the limit of asymptotically small couplings. As a result, in the weak-coupling limit the dynamics of an anisotropic QGP is dominated by the growth of unstable chromo-Weibel modes. The investigation of the evolution of soft (gauge) fields subject to dynamical instabilities such as the chromo-Weibel instability [40–52] is an active area of research. Field dynamics in an expanding background have been recently investigated using classical Yang–Mills simulations [53,54,57,63,78,117,123,124], analytically in the high-energy limit [58,59], within scalar ϕ^4 theory subject to parametric resonance instabilities [125], and SU(2) Vlasov–Yang–Mills [55,56,61] including longitudinal expansion. There have also been developments in the area of chromohydrodynamics approaches which also show the presence of the (chromo-)Weibel instability [126–128].

The BMMS parametric relation has recently been revisited by Kurkela and Moore (KM) [58,59] to include the effect of the chromo-Weibel instabilities (among many other possibilities which were extensively considered in these papers). Their conclusion in [58] was that, when putting all the pieces together, the parametric estimate of the thermalization time of the QGP changes to $\tau_{\text{therm}} \sim \alpha_{\text{s}}^{-5/2} Q_{\text{s}}^{-1}$. However, they did not provide an estimate for the constant of proportionality. In terms of the exponent of α_{s}, one finds in the BMSS scenario $13/5 = 2.6$ and in the KM scenario one finds instead $5/2 = 2.5$. However, the uncertainty in the constant of proportionality remains, which could significantly change things. Assuming that this constant is of order 1, one finds that in the weak-coupling limit, plasma instabilities accelerate the thermalization of the QGP, but not dramatically. Once again, however, associating one number with both thermalization and isotropization is probably too limiting, because evidence to date indicates that the plasma may become thermal on a shorter time-scale than it becomes isotropic in momentum–space (at least for the soft momenta that viscous hydrodynamical modelling can reliably describe).

In the weak-field regime with a fixed momentum–space anisotropy, the chromo-Weibel instability initially causes exponential growth of transverse chromomagnetic and chromoelectric fields. However, due to the non-Abelian interaction between the fields, exponentially growing longitudinal chromomagnetic and chromoelectric fields are induced which grow at twice the rate of the transverse field configurations. Eventually, all components of the unstable gauge-field configurations become of equal magnitude. As a result, one finds strong gauge field self-interaction at late times and numerical simulations are necessary to have a firm quantitative understanding of the late-time behaviour of the system [46,51,52,54,63,116,129–139]. To understand the precise role played by the chromo-Weibel instability in ultrarelativistic heavy-ion collisions, one must include the effect of strong longitudinal expansion of the matter. For the first few fm/c of the QGP's lifetime, the longitudinal expansion dominates the transverse expansion. Therefore, to good approximation, one can understand the early time dynamics of the QGP by considering only longitudinal expansion. The first study to look at the effect of longitudinal expansion was done in the context of pure Yang–Mills dynamics initialized with CGC initial conditions onto which small-amplitude rapidity fluctuations were added [54]. The initial small-amplitude fluctuations result from quantum corrections to the classical dynamics [57,132,139]. Numerical studies have shown that adding spatial-rapidity

fluctuations results in the growth of chromomagnetic and chromoelectric fields with amplitudes $\sim\exp(2m_{\rm D}^0\sqrt{\tau/Q_{\rm s}})$ where $m_{\rm D}^0$ is the initial Debye screening mass and τ is the proper time. This growth with $\exp(\sqrt{\tau})$ was predicted by Arnold *et al* based on the fact that longitudinal expansion dilutes the density [46].

In a recent study within the hard-loop framework, Attems *et al* [61] assumed that the background particles are longitudinally free streaming and, as a result, the background (hard) particles possess a local rest frame momentum–space anisotropy which increases quadratically in proper time. Given an isotropic distribution $f_{\rm iso}$, the corresponding longitudinal free-streaming one-particle distribution function can be straightforwardly constructed. Following [55] one can obtain the dynamical equations obeyed by colour perturbations δf^a of a colour-neutral longitudinally free-streaming momenta distribution $f_0 V\cdot D\,\delta f^a\big|_{p^\mu} = gV^\mu F^a_{\mu\nu}\partial^\nu_{(p)} f_0(\mathbf{p}_\perp, p_\eta)$. This equation must be solved simultaneously together with the non-Abelian Yang–Mills equations which couple the colour-charge fluctuations back to the gauge fields via the induced colour-currents j_a^ν

$$D_\mu F_a^{\mu\nu} = j_a^\nu = g\,t_R\int\frac{{\rm d}^3p}{(2\pi)^3}\frac{p^\mu}{2p^0}\delta f_a(\mathbf{p},\mathbf{x},t)\,, \tag{2}$$

where $D_\alpha = \partial_\alpha - ig[A_\alpha,\cdot]$ is the gauge covariant derivative, $F_{\alpha\beta} = \partial_\alpha A_\beta - \partial_\beta A_\alpha - ig[A_\alpha, A_\beta]$ is the gluon field strength tensor, and g is the strong coupling. This equation is then transformed to co-moving coordinates with the metric

$${\rm d}s^2 = {\rm d}\tau^2 - {\rm d}\mathbf{x}_\perp^2 - \tau^2{\rm d}\eta^2.$$

The resulting dynamical equations are numerically solved in temporal axial gauge on a spatial lattice. To maintain gauge invariance with respect to three-dimensional gauge transformations, the spatially-discretized fields are represented by plaquette variables and evolved along with the conjugate momentum using a leap-frog algorithm. The fluctuation-induced currents are represented by auxiliary fields which are discretized in space and also on a cylindrical velocity-surface spanned by azimuthal velocity and rapidity. As a result, the simulations are effectively five-dimensional and are, therefore, computationally intensive. For details concerning the numerical implementation see ref. [61]. For the initial conditions, ref. [61] seeded current fluctuations of amplitude Δ which had a UV spectral cut-off. In figure 3a the various components of the chromofield energy density as a function of rescaled proper time $\tilde\tau$ are shown. For LHC and RHIC initial energy densities, one unit in $\tilde\tau$ corresponds to $\sim$1 fm/c and 1.4 fm/c, respectively. For this figure an initial fluctuation amplitude of $\Delta = 0.8$ was chosen.

As can be seen from this figure, after $\sim$1 fm/c, we begin to see rapid growth of the transverse chromomagetic field, followed by the transverse chromoelectric field, and then the longitudinal chromofields. In figure 3b, we show the resulting ratio of the total (particle plus field) longitudinal pressure divided by the total transverse pressure for various values of Δ. At early times, prior to unstable mode growth, one observes that the longitudinal pressure drops due to the longitudinal free streaming of the hard particle background. However, when the unstable modes have grown significantly, one observes a regeneration of the longitudinal pressure by the unstable modes. In addition, one observes that the time at which isotropy is restored is primarily sensitive to the initial fluctuation amplitude Δ.

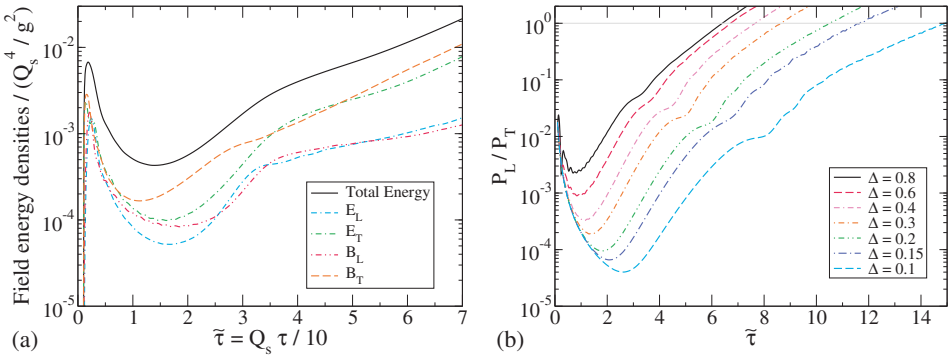

Figure 3. (**a**) The various components of the chromofield energy density as a function of proper time. (**b**) The total (field plus particle) longitudinal over transverse pressure as a function of proper time.

In addition to extracting information about the energy density and pressures of the system as a function of proper time, one can also extract information from the gauge field spectra. The longitudinal spectra can be obtained following ref. [57] by first Fourier transforming each field component, integrating over the transverse wave vectors and decomposing each according to the longitudinal wave vector ν, in terms of which the electric and magnetic energy densities are decomposed into longitudinal energy spectra (see ref. [61] for details). In figure 4 (left) the extracted longitudinal spectra, extracted using the first method averaged over 50 runs, is shown. The lines shown in the panel are fits to a form $\mathcal{E} \propto \int \mathrm{d}k_z \left(k_z^2 + 2|k_z|T + 2T^2\right) \exp(-|k_z|/T)$ which is obtained by integrating a Boltzmann distribution over transverse momenta. As can be seen from these panels, this

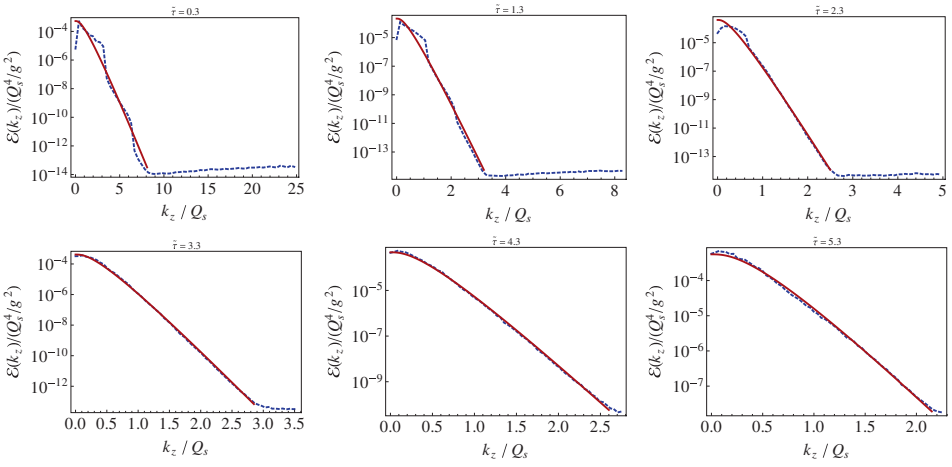

Figure 4. On the left, the longitudinal spectra at various proper times are shown. On the right, the extracted longitudinal temperature is shown which was obtained by a fit (see text) to the longitudinal spectra ($\mathcal{E}$) or the Fourier transform of the spatial energy density ($\bar{\mathcal{E}}$).

fit function begins to describe the observed spectra very well at early times corresponding to $\tilde{\tau} \sim 1$ indicating extremely fast longitudinal thermalization of the spectra even though the system is still highly anisotropic at this moment in time.

4. Conclusions and outlook

In this brief review, I have attempted to discuss recent advances and outstanding questions regarding our theoretical understanding of the thermalization and isotropization of the QGP. As pointed out herein, at this moment in time all signs indicate that the QGP created in URHICs is anisotropic in momentum–space with large anisotropies expected at early times and near the transverse edges of the plasma. These anisotropies last for multiple fm/c and, as a result, modern phenomenological approaches should include these anisotropies, e.g. production matrix elements, quark energy loss, and quarkonium potentials [140]. Despite the momentum–space anisotropy in the local rest frame, there are indications from both the weak- and strong-coupling approaches that the system thermalizes in the sense that there is (at least transiently) a Boltzmann-like distribution of energy or the formation of an apparent horizon in the bulk, respectively.

On the weak-coupling side, calculations and simulations are increasing their scope and associated complexity. The simulations required are numerically intensive due to high dimensionality, in the case of hard-loop codes, and the large lattice sizes and statistical averaging required in general. As a result, the time-scale for advances in our understanding of weak-coupling dynamics has grown longer recently. On the strong-coupling side, there have been significant advances in our understanding of strong-coupling thermalization and (an)isotropization of the QGP. The state-of-the-art calculations now include azimuthally symmetric transverse expansion for smooth initial conditions and are able to interpolate between full stopping and boost-invariant Bjorken flow based on the initial condition chosen. As these simulations become more realistic and eventually start to include fluctuations in the initial conditions, they too will face some rather daunting numerical problems, but these are not insurmountable.

Acknowledgements

This work was supported in part by DOE Grant No. DE-SC0004104.

References

[1] P Huovinen, P F Kolb, Ulrich W Heinz, P V Ruuskanen and S A Voloshin, *Phys. Lett. B* **503**, 58 (2001), hep-ph/0101136
[2] Tetsufumi Hirano and Keiichi Tsuda, *Phys. Rev. C* **66**, 054905 (2002), nucl-th/0205043
[3] M J Tannenbaum, *Rept. Prog. Phys.* **69**, 2005 (2006), nucl-ex/0603003
[4] Peter F Kolb and Ulrich W Heinz, *in: Quark gluon plasma* edited by R C Hwa *et al* (World Scientific, Singapore, 2004) pp. 634–714, nucl-th/0305084 (2003)
[5] Azwinndini Muronga, *Phys. Rev. Lett.* **88**, 062302 (2002), nucl-th/0104064
[6] Azwinndini Muronga, *Phys. Rev. C* **69**, 034903 (2004), nucl-th/0309055
[7] Azwinndini Muronga and Dirk H Rischke, nucl-th/0407114 (2004)

[8] Rudolf Baier, Paul Romatschke and Urs Achim Wiedemann, *Phys. Rev. C* **73**, 064903 (2006), hep-ph/0602249
[9] Paul Romatschke and Ulrike Romatschke, *Phys. Rev. Lett.* **99**, 172301 (2007), 0706.1522
[10] Rudolf Baier, Paul Romatschke, Dam Thanh Son, Andrei O Starinets and Mikhail A Stephanov, *J. High Energy Phys.* **04**, 100 (2008), 0712.2451
[11] K Dusling and D Teaney, *Phys. Rev. C* **77**, 034905 (2008), 0710.5932
[12] Matthew Luzum and Paul Romatschke, *Phys. Rev. C* **78**, 034915 (2008), 0804.4015
[13] Huichao Song and Ulrich W Heinz, *J. Phys. G* **36**, 064033 (2009), 0812.4274
[14] Ulrich W Heinz, *Relativistic heavy ion physics, Landolt–Boernstein new series, I/23* edited by R Stock (Springer Verlag, New York, 2010), Chap. 5, 0901.4355
[15] A El, Z Xu and C Greiner, *Phys. Rev. C* **81**, 041901 (2010), 0907.4500
[16] J Peralta-Ramos and E Calzetta, *Phys. Rev. D* **80**, 126002 (2009), 0908.2646
[17] J Peralta-Ramos and E Calzetta, *Phys. Rev. C* **82**, 054905 (2010), 1003.1091
[18] G S Denicol, T Kodama and T Koide, *J. Phys. G* **37**, 094040 (2010), 1002.2394
[19] G S Denicol, T Koide and D H Rischke, *Phys. Rev. Lett.* **105**, 162501 (2010), 1004.5013
[20] Bjorn Schenke, Sangyong Jeon and Charles Gale, *Phys. Rev. Lett.* **106**, 042301 (2011), 1009.3244
[21] Bjoern Schenke, Sangyong Jeon and Charles Gale, *Phys. Lett. B* **702**, 59 (2011), 1102.0575
[22] Chun Shen, Ulrich Heinz, Pasi Huovinen and Huichao Song, *Phys. Rev. C* **84**, 044903 (2011), 1105.3226
[23] Piotr Bozek, *Phys. Lett. B* **699**, 283 (2011), 1101.1791
[24] Harri Niemi, Gabriel S Denicol, Pasi Huovinen, Etele Molnar and Dirk H Rischke, *Phys. Rev. Lett.* **106**, 212302 (2011), 1101.2442
[25] H Niemi, G S Denicol, P Huovinen, E Molnár and D H Rischke, *Phys. Rev. C* **86**, 014909 (2012)
[26] Piotr Bożek and Iwona Wyskiel-Piekarska, *Phys. Rev. C* **85**, 064915 (2012)
[27] G S Denicol, H Niemi, E Molnár and D H Rischke, *Phys. Rev. D* **85**, 114047 (2012)
[28] Mauricio Martinez and Michael Strickland, *Nucl. Phys. A* **848**, 183 (2010), 1007.0889
[29] Wojciech Florkowski and Radoslaw Ryblewski, *Phys. Rev. C* **83**, 034907 (2011), 1007.0130
[30] Radoslaw Ryblewski and Wojciech Florkowski, *J. Phys. G* **38**, 015104 (2011), 1007.4662
[31] Mauricio Martinez and Michael Strickland, *Nucl. Phys. A* **856**, 68 (2011), 1011.3056
[32] Radoslaw Ryblewski and Wojciech Florkowski, *Eur. Phys. J. C* **71**, 1761 (2011), 1103.1260
[33] Wojciech Florkowski and Radoslaw Ryblewski, *Phys. Rev. C* **85**, 044902 (2012), 1111.5997
[34] Mauricio Martinez, Radoslaw Ryblewski and Michael Strickland, *Phys. Rev. C* **85**, 064913 (2012), 1204.1473
[35] Radoslaw Ryblewski and Wojciech Florkowski, *Phys. Rev. C* **85**, 064901 (2012), 1204.2624
[36] Wojciech Florkowski, Radoslaw Maj, Radoslaw Ryblewski and Michael Strickland, *Phys. Rev. C* **87**, 034914 (2013), 1209.3671
[37] J Peralta-Ramos and E Calzetta, *Phys. Rev. D* **87**, 3, 034003 (2013), 1212.0824
[38] Wojciech Florkowski and Radoslaw Maj, *Acta Phys. Polon. B* **44**, 10, 2003 (2013), 1309.2786
[39] Dennis Bazow, Ulrich W Heinz and Michael Strickland, 1311.6720 (2013), *Phys. Rev. C* **90**, 054910 (2014)
[40] Ulrich W Heinz, *Nucl. Phys. A* **418**, 603C (1984)
[41] Stanislaw Mrowczynski, *Phys. Lett. B* **214**, 587 (1988)
[42] Yu E Pokrovsky and A V Selikhov, *JETP Lett.* **47**, 12 (1988)
[43] S Mrowczynski, *Phys. Lett. B* **314**, 118 (1993)
[44] Jean-Paul Blaizot and Edmond Iancu, *Phys. Rept.* **359**, 355 (2002), hep-ph/0101103
[45] Paul Romatschke and Michael Strickland, *Phys. Rev. D* **68**, 036004 (2003), hep-ph/0304092
[46] Peter Brockway Arnold, Jonathan Lenaghan and Guy D Moore, *J. High Energy Phys.* **0308**, 002 (2003), Erratum added online, sep/29/2004, hep-ph/0307325

[47] Peter Brockway Arnold and Jonathan Lenaghan, *Phys. Rev. D* **70**, 114007 (2004), hep-ph/0408052
[48] Paul Romatschke and Michael Strickland, *Phys. Rev. D* **70**, 116006 (2004), hep-ph/0406188
[49] Peter Arnold, Jonathan Lenaghan, Guy D Moore and Laurence G Yaffe, *Phys. Rev. Lett.* **94**, 072302 (2005), nucl-th/0409068
[50] Stanislaw Mrowczynski, Anton Rebhan and Michael Strickland, *Phys. Rev. D* **70**, 025004 (2004), hep-ph/0403256
[51] Anton Rebhan, Paul Romatschke and Michael Strickland, *Phys. Rev. Lett.* **94**, 102303 (2005), hep-ph/0412016
[52] Anton Rebhan, Paul Romatschke and Michael Strickland, *J. High Energy Phys.* **09**, 041 (2005), hep-ph/0505261
[53] Paul Romatschke and Raju Venugopalan, *Phys. Rev. Lett.* **96**, 062302 (2006), hep-ph/0510121
[54] Paul Romatschke and Raju Venugopalan, *Phys. Rev. D* **74**, 045011 (2006), hep-ph/0605045
[55] Paul Romatschke and Anton Rebhan, *Phys. Rev. Lett.* **97**, 252301 (2006), hep-ph/0605064
[56] Anton Rebhan, Michael Strickland and Maximilian Attems, *Phys. Rev. D* **78**, 045023 (2008), 0802.1714
[57] Kenji Fukushima and Francois Gelis, *Nucl. Phys. A* **874**, 108 (2012), 1106.1396
[58] Aleksi Kurkela and Guy D Moore, *J. High Energy Phys.* **1112**, 044 (2011), 1107.5050
[59] Aleksi Kurkela and Guy D Moore, *J. High Energy Phys.* **1111**, 120 (2011), 1108.4684
[60] Jean-Paul Blaizot, Francois Gelis, Jin-Feng Liao, Larry McLerran and Raju Venugopalan, *Nucl. Phys. A* **873**, 68 (2012), 1107.5296
[61] Maximilian Attems, Anton Rebhan and Michael Strickland, *Phys. Rev. D* **87**, 025010 (2013), 1207.5795
[62] Aleksi Kurkela and Guy D Moore, 1209.4091 (2012)
[63] Jurgen Berges, Kirill Boguslavski and Soren Schlichting, *Phys. Rev. D* **85**, 076005 (2012), 1201.3582
[64] Jean-Paul Blaizot, Jinfeng Liao and Larry McLerran, *Nucl. Phys. A* **920**, 58 (2013), 1305.2119
[65] Paul M Chesler and Laurence G Yaffe, *Phys. Rev. Lett.* **102**, 211601 (2009), 0812.2053
[66] Daniel Grumiller and Paul Romatschke, *J. High Energy Phys.* **0808**, 027 (2008), 0803.3226
[67] Paul M Chesler and Laurence G Yaffe, *Phys. Rev. D* **82**, 026006 (2010), 0906.4426
[68] Javier L Albacete, Yuri V Kovchegov and Anastasios Taliotis, *J. High Energy Phys.* **0905**, 060 (2009), 0902.3046
[69] Bin Wu and Paul Romatschke, *Int. J. Mod. Phys. C* **22**, 1317 (2011), 1108.3715
[70] Michal P Heller, Romuald A Janik and Przemyslaw Witaszczyk, *Phys. Rev. Lett.* **108**, 201602 (2012), 1103.3452
[71] Paul M Chesler and Derek Teaney, 1112.6196 (2011)
[72] Michal P Heller, Romuald A Janik and Przemyslaw Witaszczyk, *Phys. Rev. D* **85**, 126002 (2012), 1203.0755
[73] Wilke van der Schee, *Phys. Rev. D* **87**, 061901 (2013), 1211.2218
[74] Paul Romatschke and J Drew Hogg, *J. High Energy Phys.* **1304**, 048 (2013), 1301.2635
[75] Jorge Casalderrey-Solana, Michal P Heller, David Mateos and Wilke van der Schee, *Phys. Rev. Lett.* **111**, 181601 (2013), 1305.4919
[76] Wilke van der Schee, Paul Romatschke and Scott Pratt, *Phys. Rev. Lett.* **111**, 222302 (2013), 1307.2539
[77] J Berges, K Boguslavski, S Schlichting and R Venugopalan, 1303.5650 (2013), *Phys. Rev. D* **89**, 074011 (2014)
[78] Juergen Berges, Kirill Boguslavski, Soeren Schlichting and Raju Venugopalan, 1311.3005 (2013), *Phys. Rev. D* **89**, 114007 (2014)

[79] Paul Romatschke and Michael Strickland, *Phys. Rev. D* **69**, 065005 (2004), hep-ph/0309093
[80] Paul Romatschke and Michael Strickland, *Phys. Rev. D* **71**, 125008 (2005), hep-ph/0408275
[81] Bjorn Schenke and Michael Strickland, *Phys. Rev. D* **76**, 025023 (2007), hep-ph/0611332
[82] Mauricio Martinez and Michael Strickland, *Phys. Rev. Lett.* **100**, 102301 (2008), 0709.3576
[83] Mauricio Martinez and Michael Strickland, *Phys. Rev. C* **78**, 034917 (2008), 0805.4552
[84] Adrian Dumitru, Yasushi Nara, Bjoern Schenke and Michael Strickland, *Phys. Rev. C* **78**, 024909 (2008), 0710.1223
[85] Adrian Dumitru, Yun Guo and Michael Strickland, *Phys. Lett. B* **662**, 37 (2008), 0711.4722
[86] Lusaka Bhattacharya and Pradip Roy, 0809.4596 (2008)
[87] Lusaka Bhattacharya and Pradip Roy, *Phys. Rev. C* **79**, 054910 (2009), 0812.1478
[88] Adrian Dumitru, Yun Guo, Agnes Mocsy and Michael Strickland, *Phys. Rev. D* **79**, 054019 (2009), 0901.1998
[89] Y Burnier, M Laine and M Vepsalainen, *Phys. Lett. B* **678**, 86 (2009), 0903.3467
[90] Adrian Dumitru, Yun Guo and Michael Strickland, *Phys. Rev. D* **79**, 114003 (2009), 0903.4703
[91] Owe Philipsen and Marcus Tassler, 0908.1746 (2009)
[92] Lusaka Bhattacharya and Pradip Roy, *Phys. Rev. C* **81**, 054904 (2010), 0907.3607
[93] Lusaka Bhattacharya and Pradip Roy, *J. Phys. G* **37**, 105010 (2010), 1001.1054
[94] Matthew Margotta, Kyle McCarty, Christina McGahan, Michael Strickland and David Yager-Elorriaga, *Phys. Rev. D* **83**, 105019 (2011), 1101.4651
[95] Michael Strickland, *Phys. Rev. Lett.* **107**, 132301 (2011), 1106.2571
[96] Michael Strickland and Dennis Bazow, *Nucl. Phys. A* **879**, 25 (2012), 1112.2761
[97] Mahatsab Mandal, Lusaka Bhattacharya and Pradip Roy, *Phys. Rev. C* **84**, 044910 (2011), 1101.5855
[98] Mahatsab Mandal and Pradip Roy, *Phys. Rev. C* **86**, 024915 (2012), 1105.5528
[99] Michael Strickland, *AIP Conf. Proc.* **1520**, 179 (2013), 1207.5327
[100] Wojciech Florkowski, Radoslaw Ryblewski and Michael Strickland, *Phys. Rev. D* **86**, 085023 (2012)
[101] Mahatsab Mandal and Pradip Roy, *Adv. High Energy Phys.* **2013**, 371908 (2013)
[102] Kevin Dusling and Shu Lin, *Nucl. Phys. A* **809**, 246 (2008), 0803.1262
[103] Kevin Dusling, 0901.2027 (2008)
[104] Maxime Dion, Jean-Francois Paquet, Bjorn Schenke, Clint Young, Sangyong Jeon *et al*, *Phys. Rev. C* **84**, 064901 (2011), 1109.4405
[105] Chun Shen, Ulrich W Heinz, Jean-Francois Paquet, Igor Kozlov and Charles Gale, 1308.2111 (2013), *Phys. Rev. C* **91**, 024908 (2015)
[106] Chun Shen, Ulrich W Heinz, Jean-Francois Paquet and Charles Gale, 1308.2440 (2013), *Phys. Rev. C* **89**, 044910 (2014)
[107] Gojko Vujanovic, Clint Young, Bjoern Schenke, Ralf Rapp, Sangyong Jeon *et al*, 1312.0676 (2013), *Phys. Rev. C* **89**, 034904 (2014)
[108] G Policastro, D T Son and A O Starinets, *Phys. Rev. Lett.* **87**, 081601 (2001), hep-th/0104066
[109] Sayantani Bhattacharyya, Veronika E Hubeny, Shiraz Minwalla and Mukund Rangamani, *J. High Energy Phys.* **02**, 045 (2008), 0712.2456
[109a] A similar time-scale emerges within the kinetic theory framework.
[109b] For this figure, the transport coefficient $\lambda_1 = 0$ is taken. In figure 13 of ref. [110] one can find a comparison plot including non-vanishing λ_1.
[110] Wojciech Florkowski, Radoslaw Ryblewski and Michael Strickland, 1305.7234 (2013), *Phys. Rev. C* **88**, 024903 (2013)
[111] Charles Gale, Sangyong Jeon, Bjorn Schenke, Prithwish Tribedy and Raju Venugopalan, *Phys. Rev. Lett.* **110**, 012302 (2013), 1209.6330

[112] Larry D McLerran and Raju Venugopalan, *Phys. Rev. D* **49**, 2233 (1994), hep-ph/9309289
[113] Larry D McLerran and Raju Venugopalan, *Phys. Rev. D* **49**, 3352 (1994), hep-ph/9311205
[114] Edmond Iancu and Raju Venugopalan, hep-ph/0303204 (2003)
[114a] At $\tau = 0^+$, the longitudinal pressure is negative due to coherent field effects; however, within a few fractions of a fm/c it becomes positive and at leading order goes to zero rapidly.
[115] Michael Strickland, *J. Phys. G* **34**, S429 (2007), hep-ph/0701238
[116] Juergen Berges, Sebastian Scheffler and Denes Sexty, *Phys. Rev. D* **77**, 034504 (2008), 0712.3514
[117] Thomas Epelbaum and Francois Gelis, *Phys. Rev. Lett.* **111**, 232301 (2013), 1307.2214
[118] R Baier, Alfred H Mueller, D Schiff and D T Son, *Phys. Lett. B* **502**, 51 (2001), hep-ph/0009237
[119] Alex Krasnitz, Yasushi Nara and Raju Venugopalan, *Phys. Rev. Lett.* **87**, 192302 (2001), hep-ph/0108092
[119a] This instability is named in reference to the analogous Weibel instability which exists in Abelian electromagnetic plasmas [120].
[120] Erich S Weibel, *Phys. Rev. Lett.* **2**, 83 (1959)
[121] Stanislaw Mrowczynski and Markus H Thoma, *Phys. Rev. D* **62**, 036011 (2000), hep-ph/0001164
[122] Bjorn Schenke and Michael Strickland, *Phys. Rev. D* **74**, 065004 (2006), hep-ph/0606160
[123] Kenji Fukushima, *Acta Phys. Polon. B* **42**, 2697 (2011), 1111.1025
[124] Kenji Fukushima, 1307.1046 (2013), *Phys. Rev. C* **89**, 024907 (2014)
[125] Kevin Dusling, Thomas Epelbaum, Francois Gelis and Raju Venugopalan, *Phys. Rev. D* **86**, 085040 (2012), 1206.3336
[126] B Basu, *Phys. Plasmas (1994–present)* **9**, 12, 5131 (2002)
[127] Cristina Manuel and Stanislaw Mrówczyński, *Phys. Rev. D* **74**, 105003 (2006), hep-ph/0606276
[128] E Calzetta and J Peralta-Ramos, 1309.5412 (2013)
[129] Peter Brockway Arnold, Guy D Moore and Laurence G Yaffe, *Phys. Rev. D* **72**, 054003 (2005), hep-ph/0505212
[130] Peter Brockway Arnold and Guy D Moore, *Phys. Rev. D* **73**, 025006 (2006), hep-ph/0509206
[131] Peter Brockway Arnold and Guy D Moore, *Phys. Rev. D* **73**, 025013 (2006), hep-ph/0509226
[132] Kenji Fukushima, Francois Gelis and Larry McLerran, *Nucl. Phys. A* **786**, 107 (2007), hep-ph/0610416
[133] Dietrich Bodeker and Kari Rummukainen, *J. High Energy Phys.* **0707**, 022 (2007), 0705.0180
[134] Peter Brockway Arnold and Guy D Moore, *Phys. Rev. D* **76**, 045009 (2007), 0706.0490
[135] J Berges, S Scheffler and D Sexty, *Phys. Lett. B* **681**, 362 (2009), 0811.4293
[136] Juergen Berges, Daniil Gelfand, Sebastian Scheffler and Denes Sexty, *Phys. Lett. B* **677**, 210 (2009), 0812.3859
[137] Juergen Berges, Jens Pruschke and Alexander Rothkopf, *Phys. Rev. D* **80**, 023522 (2009), 0904.3073
[138] Andreas Ipp, Anton Rebhan and Michael Strickland, *Phys. Rev. D* **84**, 056003 (2011), 1012.0298
[139] Kevin Dusling, Francois Gelis and Raju Venugopalan, *Nucl. Phys. A* **872**, 161 (2011), 1106.3927
[140] In the context of viscous hydrodynamics, this translates into including the viscous corrections to the thermal one-particle distribution function self-consistently in the hydrodynamic simulation as well as the process under consideration.